# A dual-functional microfluidic chip for on-line detection of interleukin-8 based on rolling circle amplification

Wanling Zhang, Ziyi He, Linglu Yi, Sifeng Mao, Haifang Li, Jin-Ming Lin

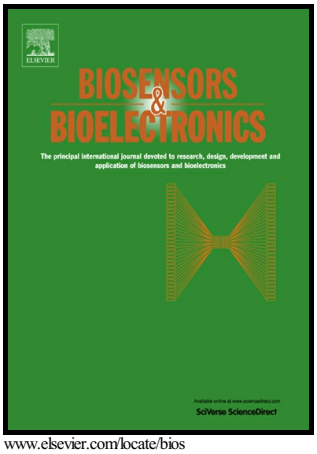


www.elsevier.com/locate/bios

PII: S0956-5663(17)30815-1
DOI: https://doi.org/10.1016/j.bios.2017.12.017
Reference: BIOS10162

To appear in: *Biosensors and Bioelectronic*

Received date: 2 October 2017
Revised date: 23 November 2017
Accepted date: 11 December 2017

Cite this article as: Wanling Zhang, Ziyi He, Linglu Yi, Sifeng Mao, Haifang Li and Jin-Ming Lin, A dual-functional microfluidic chip for on-line detection of interleukin-8 based on rolling circle amplification, *Biosensors and Bioelectronic,* https://doi.org/10.1016/j.bios.2017.12.017

# A dual-functional microfluidic chip for on-line detection of interleukin-8 based on rolling circle amplification

**Wanling Zhang, Ziyi He, Linglu Yi, Sifeng Mao, Haifang Li, Jin-Ming Lin***

Department of Chemistry, Beijing Key Laboratory of Microanalytical Methods and Instrumentation, MOE Key Laboratory of Bioorganic Phosphorus Chemistry & Chemical Biology, Tsinghua University, Beijing 100084, People's Republic of China

*Corresponding Author:
Prof. Dr. Jin-Ming Lin
Department of Chemistry
Tsinghua University
Beijing 100084
**Tel:** 0086-10-62792343
**E-mail:** jmlin@mail.tsinghua.edu.cn

**Keywords:** microfluidic chip; aptamer; rolling circle amplification; interleukin-8; glioma stem-like cells

## Abstract

Interleukin 8 (IL-8), also known as C-X-C motif ligand 8(CXCL8), is a proinflammatory chemokine functioned in neutrophil chemotaxis and activation. And it plays an important role in the process of glioma stem-like cell vascularization in the latest research. Herein, a dual-function microfluidic biosensor based on rolling circle amplification (RCA) was fabricated for cell culture and online IL-8 detection. A microfluidic chip was designed with two high passages connected by the vertical channels. One of the channels with immobilized capture antibody was prepared for IL-8 detection and another channel for cell culture. Immunoassays were achieved by a sandwich structure consisting of antibodies, IL-8, and aptamers. Signal amplification was mainly due to RCA and biotin-streptavidin linkage. The linear range for IL-8 was 7.5 -120 pg•mL$^{-1}$ in this assay. Moreover, the developed method was successfully applied to detect the IL-8 in tumor-derived endothelial cells (TDEC) and Human Umbilical Vein Endothelial cells (HUVEC) under chemical hypoxia condition. Semi-quantitative detection of IL-8 consumption in HUVEC cells in low oxygen condition was also achieved. These results were in statistical agreement with those obtained by commercial assay of enzyme-linked immunoassay kit (ELISA). The microfluidic chip based biosensor reported hereby has a large prospect in the basic research and clinical diagnosis of cancer stem cell.

## 1. Introduction

Glioblastomas (GBMs) are the most lethal malignancy in the human tumor. An important feature of glioma is the abundant and highly aberrant vascular system, thus there are increasing interest in angiogenesis process in GBMs. (Hardee and Zagzag 2012) The recent researches demonstrate that a significant portion of the vascular endothelium has a neoplastic origin, and the glioblastomas stem-like cells (GSCs) have the potential of transdifferentiating to endothelial like cells(Ricci-Vitiani et al. 2010; Soda and Hanahan 2011). This transdifferentiation process involves a series of cytokines, including vascular endothelial growth factor (VEGF), transforming growth factor beta, and interleukin-8（IL-8）(Brat et al. 2005; Joseph et al. 2014; Zhao et al. 2010). IL-8 is a chemokine with a defining CXC motif secreted by many kinds of cells. CXC means that this chemokine was has two N-terminal cysteines separated by an amino acid. Now it is also known for possessing tumorigenic and proangiogenic properties(Waugh and Wilson 2008). In human gliomas, IL-8 is expressed and secreted at high levels both in vitro and in vivo(Shi and Wei 2016). The level of IL-8 is associated with the histological grade of glioma, and the most malignant form of glioblastoma shows the highest expression in necrotic cells, suggesting that hypoxia conditions may stimulate IL-8 expression(Brat et al. 2005). And in a glioma niche, endothelial cells and TDEC can be stimulated by IL-8 in hypoxia condition(Li et al. 2003).

Recently, diverse methods have been developed for IL-8 detection. The most common and commercialized method is the enzyme-linked immunoassay kit. The detection limit(DL) is approximately 10 $pg \cdot mL^{-1}$(Rusling et al. 2010). Fluorescence method can qualitatively detect 1 pM IL-8(Konry et al. 2009). Surface plasmon resonance is a label free detection method, with the DL of 184pM in saliva (Yang et al. 2005). Combined with nanotechnology, the DL of these methods can be further decreased to fM (Munge et al. 2011; Torrente-Rodriguez et al. 2016). There is another rapid label-free profiling of IL-8 using nano-Ultra Performance Liquid Chromatography- Quadrupole-Time of Flight (nano-UPLC-Q-TOF) ion mobility

mass spectrometry (Nassar et al. 2016). A lot of methods are concerning about the detection of IL-8 (Dong and Pires 2017). Compared with conventional protein detection method, our method is much economical and convenient, for aptamers could be easily synthesized, and they are stable under different experimental conditions (Alsaafin and McKeague 2017; Lin et al. 2015a). Although most of the fluorescence detection methods are semi-quantitative, our result could reach a linear relationship. Moreover, complex operation and expensive equipment are required by these methods. Biosensors have been greatly developed for clinical applications, because of its low cost, high selectivity and accuracy, and minimal technical experience requirements. Multiple types of biosensors have been utilized for the analysis of tumor markers such as interleukin-8, interleukin 6 and vascular endothelial growth factor, but they either have low sensitivity or are rarely able to be tested online.(Malhotra et al. 2012; Wan et al. 2011; Wei et al. 2009)

Herein, we developed an integrated microfluidic biosensor, which can simultaneously achieve the cell culture, morphology observation and IL-8 protein detection. The microfluidic chip was designed with two high channels connected by several narrow channels. Cells were cultured in one of the main channels. A sandwich-type immunoassay was designed and optimized by Bio-layer Interferometry (BLI), indicating the simultaneous binding ability of the antibody and RNA aptamer to the IL-8 protein. We modified the antibodies in the other channel for IL-8 capture. For IL-8 detection, the biotinylated RNA aptamer was bound to the captured proteins and RCA was then performed for signal amplification. The amplification effect allowed the quantitative detection of IL-8, in the linear range of 7.5-120 pg•mL$^{-1}$ (0.84 pM-13.44 pM). Through this ultrasensitive strategy, we found that the IL-8 secreted by TDEC was lower than that of HUVEC. And chemical hypoxia condition could increase the IL-8 secretion. We also demonstrated that HUVEC increased IL-8 consumption under low oxygen signal stimulation. These results confirmed that we had developed a microfluidic biosensor which is promising in the disease diagnosis. And this “sandwich” structure may also be applicable in matrix-assisted laser desorption/ionization mass spectrometry (MALDI-MS)(He et al. 2016).

## 2. Experimental

### *2.1. Materials and reagents*

Capture antibody of Interleukin-8 was purchased from Abcam (Cambridge, UK). Recombinant Human Interleukin-8 (IL-8), epidermal growth factor (EGF), basic Fibroblast Growth Factor (bFGF), VEGF，bovine serum albumin (BSA) were purchased from Pepro Tech (Rehovot, Israel). B-27 Supplement (B27), Sulfo-NHS-Biotin was purchased from Thermo Fisher (Waltham, MA, USA.) The RNA aptamer for IL-8 (5'Biotinylated–GGGGGCUUAUCAUUCCAUUUAGUGUUAUGAUAAC C-3',2'Omemodified,) was synthesized by Gene Pharma (Shanghai, China). Biotinylated RCA primer (5'Biotinylated-CCCTCAGATAGCTTATCAGACTGATG TTGACC) (Sung et al. 2014), padlock probe (5'-phosphorylated-CTGATAAGCTATC ACTATGGTCGCGCTAGGTCTATTTAGTGGAGCCCAAGTACTCACTATGGTCG CGCTAGGTCAACATCAGT) were synthesized by Synbio Tech (Suzhou, China). Phosphate buffer saline (PBS), deferoxamine mesylate（DFO）, avidin, Concanavalin A(CoA) was obtained from Sigma Aldrich Chemical Co.(St. Louis, MO, USA). Insulin, human serum albumin (HSA), adenosine triphosphate (ATP) were purchased from Solarbio, China. Phi29 DNA polymerase and deoxyribonucleoside 5'-triphosphate mixture (dNTPs), T4 ligase (New England Biolabs, UK) were essential for the rolling circle amplification (RCA) reaction. DMEM/F-12, RPMI medium 1640 (Gibco, 40 Grand Island, NY) and trypsin EDTA (Gibco, Grand Island) were purchased from Invitrogen (CA, USA). U87MG and HUVEC cells were purchased from Cancer Institute & Hospital Chinese Academy of Medical Science (Beijing, China). (3-Aminopropyl) tetraethoxysilane (APTES) (TCI, Shanghai, China) and glutaraldehyde (SCR, Beijing, China) were used to modify the microchannel. All reagents were used without further purification. The enzyme -linked immunosorbent assay kit of human interleukin 8 was purchased from Donggeweiye (Beijing, China).

An Atomic Force Microscope (Bruker, USA) was used to observe the morphology of the channel bottom. To get a comparison of aptamer-protein-antibody structure

forming sequence, we use the Bio-layer Interferometry (Octet RED96, Pall ForteBio, USA). Hypoxia chamber for cell culture was bought from Billups-Rothenberg, USA. The fluorescence images of the channel were taken by a confocal microscope (spinning disk, UltraView Vox, USA). The ELISA results were got from Multi - functional microplate reader (PerkinElmer, USA). DNA chip electrophoresis was done by MultiNA (Shimadzu, Japan). ImageJ software was got from National Institutes of Health, USA.

### *2.2. Cell culture and transdifferentiation process*

The glioblastoma cell U87MG and endothelial cells HUVEC were chosen for our experiment. All the cells were cultured in 37℃ in the cell culture incubator with 5% $CO_2$, 21%$O_2$. HUVEC was cultured in RPMI 1640, with additional 10% fetal bovine serum (FBS), and 100 U $mL^{-1}$ streptomycin, 100 U·$mL^{-1}$ penicillin. The U87MG cells were cultured in MEM medium. To get GSCs, the U87MG cells were digested and centrifuged, then resuspended in the DMEM/F-12 culture medium, with 20 ng $mL^{-1}$ FGF, 20 ng·$mL^{-1}$ EGF, 2% B27, 100 U·$mL^{-1}$ streptomycin, 100 U·$mL^{-1}$ penicillin (Li et al. 2017). B-27 supplement is an optimized serum-free supplement used to support the growth and viability of central nervous system (CNS) neurons. Then the GSC were treated with 200 UM deferoxamine mesylate (DFO) in the 21%$O_2$ in the endothelial differentiation medium (DMEM/F12 containing 0.01 μg·$mL^{-1}$ VEGF，0.01 ug·$mL^{-1}$ EGF, 0.005 μg·$mL^{-1}$ bFGF, 10% FBS, 2% B27). After 48h, we could get TDECs. Chemical hypoxia was achieved by the addition of 200 um DFO drugs, which could block proline hydroxylase to stabilize HIF-1α (Ivan et al. 2001; Jaakkola et al. 2001). The physical hypoxia condition was achieved by placing the cell culture chip in an oxygen-deficient chamber with 1.5%$O_2$, 5%$CO_2$ and 93.5% $N_2$.

### *2.3. Identification of glioma stem cells and TDECs*

The dedifferentiation and transdifferentiating result was confirmed by immunofluorescence staining. 1% polylysine was added to the confocal dish at 37 ° C for 15 min. This makes the small dish easy to adhere to the GSC ball. The medium

was aspirated and slowly added to the confocal dish. And then put the dish into the cell incubator, put it aside for 6 hours. So that GSCs adhere to the ball. Then we used 4% paraformaldehyde to treat the cells at 37 ° C for 15 min. 1 mL PBS solution was used to wash the cells for 3 times. the immunofluorescence blocking solution 1 mL was used to cell at room temperature for 1 h. 50 μL of CD133 (200-fold dilution) and 50 μL of Nestin (200 μl dilution) were added and incubated at 4 ° C for 12 h. 200 μL goat anti-mouse (CD133) and goat anti-rabbit (Nestin) were added and incubated at 37 ° C for 1 h. And then we added 200 μL DAPI staining. After repeated washing step, cells were observed under laser scanning confocal microscopy. To identify transdifferentiation results, medium was discarded and cells were washed three-times with PBS. After fluorescence blocking solution 1 mL at room temperature for 1 hour, the cells were washed with PBS again. After the incubation of the first antibody overnight and second antibody (1 h), the images were taken by laser scanning confocal microscopy.

### *2.4. Aptamer-IL-8-antibody structure optimization*

To get a better "sandwich" structure, the binding affinity of "fixed aptamer-IL-8-antibody" procedure and "fixed antibody –IL-8-aptamer" was compared by using the Bio-layer Interferometry and supplementary avidin sensors (Toh et al. 2015). And the antibody (1 $\mu g \cdot mL^{-1}$) was biotinylated by the addition n of Sulfo-NHS-Biotin reagent (100 μM) for 30 min. The reactant was purified by a 3 kDa ultra centrifugal filter. Then the biotinylated antibody solution, PBS solution, IL-8 solution, PBS solution, aptamer solution (1μM), PBS solution, each 200 μL, was added one by one in a 96- well plate. Then the 96-well plate was put into the Bio-layer Interferometry. The "fixed aptamer-IL-8-antibody" procedure binding affinity was also got from the same operation as mentioned above.

### *2.5. Chip modification*

First, the PDMS microchip was manufactured as in our previous work (Jie et al. 2016). We designed an SU-8 patterned silicon wafer with multiple parallel

micro-channels, and every channel had a volume of 5 μL. And we also designed a cell culture-detecting microfluidic chip, which had an altitude intercept of 100 um. This altitude intercept was sufficient to maintain the pressure difference on both sides of the liquid to prevent the liquid from flowing out (Lin et al. 2015b). Clean glass pieces were heated in $H_2SO_4/H_2O_2$ mixed solution (Volume ratio, 3:1) at 95℃ for one hour. Then the glass was washed with deionized water thrice. The dried glass pieces and the PDMS layer were put into plasma cleaner, then they were bonded together. After drying in the oven for 2 h at 65℃, the channels were soaked in APTES solution (2% diluted in acetone) for one hour. Then the channels were washed with acetone and deionized water thrice. After drying in an oven for 30 min, the channels were soaked in glutaraldehyde solution (5% diluted in PBS) for one hour. After this step, the channels were washed by deionized water and dried. Finally, the IL-8 antibody solution was added into the channels. After incubating in 37℃ for 15 min, the antibody solution was removed by PBS washing. Now the channels bottom are modified with antibodies and are ready to catch the IL-8 protein molecule.

### *2.6. Preparation of the aptamer-primer-circle template*

Padlock DNA (30 μM, 2.00 μL) and ligation template (90 μM, 4.00 μL) were heated to 85℃ for 5 min and then slowly cooled down to room temperature. The solution contained 1.00 μL T4 DNA enzyme (400 U/μL), 5.00 μL 0.1 mg/mL BSA, 5.00 μL of 10 × ligase buffer, and 33 μL of ultrapure water was added to the DNA solution. The mixture solution was incubated for 24h at room temperature (Lin et al. 2014).

### *2.7. RCA reaction and IL-8 detection*

After different concentration of IL-8 or cell culture medium was added into the channels, the chip was incubated in 37℃ for 15 min. Then the channels were washed with PBS for 3 times. Then this step was repeated for incubation of IL-8. Then, the RCA reaction was carried out at 37℃ for 15 min in 1μL phi29 (1 $U \cdot \mu L^{-1}$) polymerase, 1μL dNTP (10 nM), 1μL BSA (0.1 $mg \cdot mL^{-1}$), 1 μL phi29 buffer [50 mM Tris·HCl, 10

mM $MgCl_2$, 10 mM $(NH_4)_2SO_4$, pH 7.5], 20 nM DNA template (Lin et al. 2014). After ligation, the channels were washed for 3 times in PBS. Finally, the DNA probe was added into the channels.

The connection channels and the cell culture/detection channels on this biosensor had a height difference of 100 μm, resulting in a pressure difference that allows the medium to flow only in the culture channel. When detection was required, small columns were used to block the outlet of the cell culture channel. At this time, the liquid could flow through the connecting fine channel into the detection channel. Then the antibody in the assay channel captured IL-8 in the culture medium for subsequent detection. Since serum contains IL-8, we replaced the medium with 1% fetal bovine serum after adherence to the cells. To detect IL-8 secreted by TDEC cells and HUVEC cells in chemical hypoxia condition, cells were cultivated in microfluidic channels. After the addition of DFO for 24 h , the culture medium of the cell culture channel was uniformly mixed with the same volume of empty medium，then pushed into the detection channel.

### *2.8. Imaging and counting*

The chips were observed with a confocal laser scanning microscope. Cy3 Fluorescence (excitation 550/emission 561) was monitored to evaluate the concentration of IL-8. And the signal images were taken using a 200 ms image exposure time and 20 × magnification. Then the pictures were treated with ImageJ software to get a numeral result.

## 3. Result and discussion

### *3.1. Analytical concept of online IL-8 detecting biosensor*

As shown in Fig. 1A, microchannel was modified with capture antibody in advance. Then the sample was introduced into the microchannel. After incubation, the target protein was specifically captured by the antibody. The aptamer could also recognize the target protein, then primer-template complexes were linked to aptamers

by avidin-biotin interaction. Finally, Phi29 DNA polymerase was added for isothermal amplification. After adding DNA probes which were complementary to the amplified sequence and washing, only the annealing probes were left in the channel. Thus the fluorescence intensity could represent the concentration of the IL-8 protein. To observe the cell morphology at the same time, the microchip was divided into two parts by the low channels. One of the high channels was used for cell culture and drug stimulation, allowing the cells to secrete IL-8 (Fig.1B). Another high channel was used for IL-8 detection. We used this method to study the changes in IL-8 in TDEC and HUVEC under hypoxia condition, the estimated mechanism was shown as Fig. 1C. The hypoxia signal might increase the expression of IL-8 in TDEC through downstream transcription factors. The hypoxia signal upregulated the IL-8 receptor expression on the HUVEC cell surface, thereby promoting the consumption of IL-8 in the culture medium.

**Figure 1**

### *3.2. **Identification of GSCs and TDECs***

TDECs originated from tumor-initiating cells and did not result from cell fusion of ECs and tumor cells, and they have characteristics of endothelial cells. We demonstrated that TDEC could also secrete IL-8(Ouchi et al. 2016). To confirm successful transformation of glioma cells into glioma stem cells, we used immunofluorescence staining. As shown in Fig. 2A, cells grew from adherent state to suspended state, and aggregated into clusters. And the stem cell markers CD133 and nestin were highly expressed. These results indicated that the cells already had the potential of differentiation. After the stimulation of transdifferentiation culture medium and hypoxia environment, the cells returned to be adherent. By the identification of endothelial cell marker CD31, we confirmed that we obtained cells with endothelial cell traits (Fig. 2B, C and D). The cells obtained would be compared with HUVEC in subsequent experiments.

**Figure 2**

### *3.3. Characterization of microchannel modification*

To verify that we made a successful modification of microchannels (Fig.3A), we used the AFM to observe the glass bottom at a nanometer scale. Firstly, microchannels were modified by APTES, after which the glass bottom was covered with amidogen. Then IL-8 antibody was immobilized using Schiff base reaction through a glutaraldehyde linker. Recent researches commonly immobilized antibody on a surface via the modification of its carboxyl groups. (Stobiecka et al. 2016; Stobiecka and Hepel 2011). However，in this method, the sensitivity was limited by the aptamer. And the glutaraldehyde linker is much more easier to bond to amino group of antibody without activation. As shown in Fig. 3B, the blank glass had a smooth surface. After APTES treatment, glass surface could be observed with tiny ups and downs. And the modification of glutaraldehyde further increased the roughness of the surface. The addition of macromolecule, IL-8 antibody (9 kD), significantly increased the roughness of the microchannel surface, and the peak height increased to 60 nm. These results indicated that we had successfully modified the IL-8 antibody on the channel surface.

**Figure 3**

### *3.4. Evaluation of Rolling circle amplification*

For signal enhancement, we chose the rolling circle amplification method, which can reduce reagent and sample consumption, accelerate reaction kinetics, and enhance the sensitivity and specificity of detection (Sarkar et al. 2016). The primer sequence of the RCA，linked to the padlock sequence in advance, was attached to the aptamer via an streptavidin linkage. After the amplification, multiple fluorescent probes complementary to the produced repetitive sequences were added to generate enhanced optical signals that can be observed by a fluorescence microscope. Compared to the traditional polymerase chain reaction, this process was free of circulating heating. The RCA reaction process was verified using the chip electrophoresis. Compared to non-RCA group, new bands with longer migration time were displayed, representing

the products of RCA reaction (Fig.4A, C). In Fig.4A, there was a broad peak with a migration time of 75 s， which indicated the pre-conjugated RCA complex. In Fig.4C, the rightmost band was the RCA product. When we added exonuclease Ⅰ into the solution, these bands disappeared (Fig.4B, D). There is a strong and widely distributed fluorescence signal in RCA group than non-RCA group. These results indicated the successful amplification procedure, which generated an enhanced signal intensity in fluorescence imaging (Fig.4E, F).

**Figure 4**

### *3.5. Antibody-IL-8 protein-aptamer procedure optimization*

To replace the antibody in traditional “sandwich" immunoassay with the aptamer, we directly measured the binding affinity of the antibody-IL-8 protein-aptamer system and the aptamer-IL-8 protein-antibody system by BLI. A long rise in the curve of the segment represented the addition of macromolecules, with several short periods of time on behalf of the buffer balancing stages. The rise of the lines indicated the thickness of biomolecule attached to the sensors.

As shown in the binding curve (Fig.5), both of the combinations displayed three stable curves, indicating the formation of stable sandwich structures. There were four groups in each combination procedure to verify the binding affinity, which were showed in different colors. However, in the aptamer-IL-8-antibody structure, the ability to capture IL-8 protein decreased. The binding line of IL-8 was very gentle, indicating that there is a weak binding of IL-8 in this step. In the antibody-IL-8-aptamer structure, the antibody had stronger affinity to IL-8 protein, showing a higher slope of the binding curve. By changing the concentration of the antibody, we could effectively improve the binding efficiency. We speculated that the main reason for these differences was the modification of the antibody or aptamer on the glass sheet surface. Antibody had more amidogen than aptamer, so it had higher binding efficiency and less interference when reacted with the aldehyde groups on the glass. And the immobilization of aptamer on glass surface might also affect the secondary structure, thus reducing its recognition ability for IL-8 protein. Therefore,

we chose the antibody-IL-8-aptamer system for the next experiment. We established a more stable sandwich binding system by optimizing the binding sequence of aptamer and antibody. The establishment of the aptamer and antibody double recognition systems required that the two recognition sites did not overlap (Guo and Kim 2012). In our design, the recognizing site in aptamer, Val63, Val66, Lys69 and Ala74 also overlapped with the possible recognized site of antibody to IL-8(Sung et al. 2014). From the result in Fig.5, we speculated that the overlap effect might be reduced by procedure optimization. And the reduced DL satisfied the detection of cell culture medium containing different concentrations of IL-8 protein.

**Figure 5**

### *3.6. Standard curve of IL-8 detection*

To validate the accuracy of the method we established, a series of IL-8 solutions were analyzed. Before the test, we optimized some parameters in this system (Fig. S1-Fig. S4). Because of the undefined linear detection range, we first analyzed the IL-8 solutions with large concentration gradient. As shown in Fig. 6A and B, with the increase of IL-8 concentration, the area of fluorescence distribution gradually increased. When the concentration was below 120 $pg \cdot mL^{-1}$, there was a good linear relationship between the fluorescence intensity and the IL-8 concentration. When the concentration increased from 120 to 1000 $pg \cdot mL^{-1}$, the florescence distribution didn't change significantly, for the capture antibody was almost saturated at 120 $pg \cdot mL^{-1}$. We set the three times of intensity of blank control as the minimum detection limit. The turning point of the curve to the horizontal line was set as the maximum detection limit. When the IL-8 concentration continues to increase, there will be a strong non-specific adsorption tendency. We found that our method has a good linearity from 7.5 to 120 $pg \cdot mL^{-1}$, with a linear correlation coefficient $R^2$ =0.9911, n=3. It was shown that our method could quantify IL-8 in this concentration range. The sensitivity of the proposed method was comparable to ELISA. Moreover, as shown in Fig. 6C, this method had good specificity, validated by low fluorescence signal from other proteins. These results demonstrated that the microfluidic immunoassay based on

antibody-IL-8-aptamer structure and RCA system could serve as a highly sensitive and selective platform for IL-8 detection.

**Figure 6**

### *3.7. Real sample analysis*

We then used the well-developed microfluidic chip to investigate the secretion of IL-8 in TDEC and HUVEC under different conditions. From Fig. 7A and B, it could be clearly seen that the expression of IL-8 in TDEC was significantly lower than that in other three groups. Because GSCs didn't secrete IL-8, the amount of IL-8 secreted by the transformed TDEC was lower than that of mature endothelial cells HUVEC. After the addition of simulated hypoxia condition drug DFO, the secretion of IL-8 in TDEC was enhanced and reached to the same level as HUVEC. Under hypoxia conditions, the TDEC spreading area was greater than in normoxia conditions. And there was aggregation phenomenon. The results obtained by our method were in a good correlation with ELISA. The high selectivity is achieved by the high selectivity of antibody and aptamer. Antibody attached to the channels has an extraordinary selecting effect. And in the practical samples, the concentrations of proteins or other biomolecules were very low. So only the target protein, IL-8, could be fixed on the chip and get a fluorescence signal. The small deviations of the values between these two methods might be due to the heterogeneity of the RCA. However, compared with ELISA, our method was more parallel. The error in the sample volume had less impact on this method. Another advantage was that our approach consumed less sample. The volume of the cell culture channel was 10 μL, while the sample volume required by ELISA was 50 μL. For continuous cell culture and protein detection, the smaller the sampling amount, the smaller the interference to the whole system.

The level of IL-8 secreted by HUVEC cells was not different from that of the control group under DFO treating. However, studies showed that chemical hypoxia caused by cobalt chloride had an effect on IL-8 secretion in endothelial cells (Kim et al. 2006). To investigate whether hypoxia affected the IL-8 metabolism of endothelial cells, we used HUVEC cells cultured in 10% FBS containing medium and prolonged

the duration of physical hypoxia stimulation. Result demonstrated that the medium contained a higher level of IL-8, which exceeded the quantitative detection range of our method (Fig .7C). Therefore we could only get semi-quantitative results. We found a significant increase in IL-8 consumption in HUVEC cells under chemical hypoxia conditions. The possible reason was that hypoxia signals promoted the expression of IL-8 receptors on the cell surface (Campbell et al. 2013; Infanger et al. 2013; Maxwell et al. 2007). And in the case of physical hypoxia, both of the HIF-1 and HIF-2 expression rose, but they had opposite effect on the regulation of IL-8 expression (Florczyk et al. 2011). We used an ELISA kit with higher DL to verify the detection, and the results of the two methods are basically the same. These results proved that our method could also be used in semi-quantitative analysis in the high concentration range (100~1000 pg $mL^{-1}$). IL-8 played an important role in regulating the proliferation, survival, and migration of endothelial cells (Li et al. 2005). The regulation of its expression under hypoxia was not only achieved by hypoxia-inducible factors, but also by other proteins, such as adiponectin (Lee et al. 2014). Thus there is great potential for further investigating this system by the proposed strategy.

**Figure 7**

## 4. Conclusion

In this study, we successfully developed a microfluidic biosensor for cell culture and on-line IL-8 analysis. Based on a sandwich-type immunoassay and rolling circle amplification, the biosensor achieved a quantitative detection limit of 0.84 pM. Semi-quantitative detection of IL-8 in cell culture medium was also realized in high concentration range. This biosensor was successfully applied to analyze the secreted IL-8 in endothelial cells, and results indicated that IL-8 secretion of TDEC cells was lower than that of HUVEC cells in normoxia condition. However, under the stimulation of hypoxia, the secretion of TDEC cells could reach to the same level of HUVEC cells. The secretion of IL-8 did not increase and the consumption increased

significantly under low oxygen treatment. Cell morphology observation was also achieved at the same time. This proposed biosensor could be extended to the detection of IL-8 in various biological systems.

## Notes

The authors declare no competing financial interest.

## Acknowledgements

This work was financially supported by the National Natural Science Foundation of China (Nos. 21435002, 81373373, 21621003) and National Key R&D Program of China (No. 2017YFC0906800).

## References

Alsaafin, A., McKeague, M., 2017. Functional nucleic acids as in vivo metabolite and ion biosensors. Biosens. Bioelectron. 94, 94-106.

Brat, D.J., Bellail, A.C., Van Meir, E.G., 2005. The role of interleukin-8 and its receptors in gliomagenesis and tumoral angiogenesis1. Neuro Oncol. 7(2), 122-133.

Campbell, L.M., Maxwell, P.J., Waugh, D.J., 2013. Rationale and Means to Target Pro-Inflammatory Interleukin-8 (CXCL8) Signaling in Cancer. Pharmaceuticals (Basel) 6(8), 929-959.

Dong, T., Pires, N.M.M., 2017. Immunodetection of salivary biomarkers by an optical microfluidic biosensor with polyethylenimine-modified polythiophene-C70 organic photodetectors. Biosens. Bioelectron. 94, 321-327.

Florczyk, U., Czauderna, S., Stachurska, A., Tertil, M., Nowak, W., Kozakowska, M., Poellinger, L., Jozkowicz, A., Loboda, A., Dulak, J., 2011. Opposite effects of HIF-1alpha and HIF-2alpha on the regulation of IL-8 expression in endothelial cells. Free Radic. Biol. Med. 51(10), 1882-1892.

Guo, L., Kim, D.H., 2012. LSPR biomolecular assay with high sensitivity induced by aptamer-antigen-antibody sandwich complex. Biosens. Bioelectron. 31(1), 567-570.

Hardee, M.E., Zagzag, D., 2012. Mechanisms of glioma-associated neovascularization. Am. J. Pathol. 181(4), 1126-1141.

He, Z., Chen, Q., Chen, F., Zhang, J., Li, H., Lin, J.-M., 2016. DNA-mediated cell surface engineering for multiplexed glycan profiling using MALDI-TOF mass spectrometry. Chem. Sci. 7(8), 5448-5452.

Infanger, D.W., Cho, Y., Lopez, B.S., Mohanan, S., Liu, S.C., Gursel, D., Boockvar, J.A., Fischbach, C., 2013. Glioblastoma stem cells are regulated by interleukin-8 signaling in a tumoral perivascular niche. Cancer Res. 73(23), 7079-7089.

Ivan, M., Kondo, K., Yang, H., Kim, W., Valiando, J., Ohh, M., Salic, A., Asara, J.M., Lane, W.S., Jr, K.W., 2001. HIFalpha targeted for VHL-mediated destruction by proline hydroxylation: implications for O2 sensing. Science 292(5516), 464-468.

Jaakkola, P., Mole, D.R., Tian, Y.M., Wilson, M.I., Gielbert, J., Gaskell, S.J., Von, K.A., Hebestreit, H.F., Mukherji, M., Schofield, C.J., 2001. Targeting of HIF-alpha to the von Hippel-Lindau ubiquitylation complex by O2-regulated prolyl hydroxylation. Science 292(5516), 468-472.

Jie, M., Li, H.-F., Lin, L., Zhang, J., Lin, J.-M., 2016. Integrated microfluidic system for cell co-culture and simulation of drug metabolism. RSC Adv. 6(59), 54564-54572.

Joseph, J.V., Conroy, S., Tomar, T., Eggens-Meijer, E., Bhat, K., Copray, S., Walenkamp, A.M., Boddeke, E., Balasubramanyian, V., Wagemakers, M., den Dunnen, W.F., Kruyt, F.A., 2014. TGF-beta is an inducer of ZEB1-dependent mesenchymal transdifferentiation in glioblastoma that is associated with tumor invasion. Cell Death Dis. 5, e1443-1456.

Kim, K.S., Rajagopal, V., Gonsalves, C., Johnson, C., Kalra, V.K., 2006. A Novel Role of Hypoxia-Inducible Factor in Cobalt Chloride- and Hypoxia-Mediated Expression of IL-8 Chemokine in Human Endothelial Cells. The Journal of Immunology 177(10), 7211-7224.

Konry, T., Hayman, R.B., Walt, D.R., 2009. Microsphere-based rolling circle amplification microarray for the detection of DNA and proteins in a single assay. Anal. Chem. 81(14), 5777-5782.

Lee, Y.A., Ji, H.I., Lee, S.H., Hong, S.J., Yang, H.I., Chul Yoo, M., Kim, K.S., 2014. The role of adiponectin in the production of IL-6, IL-8, VEGF and MMPs in human endothelial cells and osteoblasts: implications for arthritic joints. Exp. Mol. Med. 46, e72-78.

Li, A., Dubey, S., Varney, M.L., Dave, B.J., Singh, R.K., 2003. IL-8 Directly Enhanced Endothelial Cell Survival, Proliferation, and Matrix Metalloproteinases Production and Regulated Angiogenesis. The Journal of Immunology 170(6), 3369-3376.

Li, A., Varney, M.L., Valasek, J., Godfrey, M., Dave, B.J., Singh, R.K., 2005. Autocrine role of interleukin-8 in induction of endothelial cell proliferation, survival, migration and MMP-2 production and angiogenesis. Angiogenesis 8(1), 63-71.

Li, N., Yi, L., He, Z., Zhang, W., Li, H., Lin, J.M., 2017. A DNA-directed covalent conjugation fluorescence probe for in vitro detection of functional matrix metalloproteinases. Analyst 142, 634-640.

Lin, X., Chen, Q., Liu, W., Li, H., Lin, J.M., 2014. A portable microchip for ultrasensitive and high-throughput assay of thrombin by rolling circle amplification and hemin/G-quadruplex system. Biosens. Bioelectron. 56, 71-76.

Lin, X., Chen, Q., Liu, W., Yi, L., Li, H., Wang, Z., Lin, J.M., 2015a. Assay of multiplex proteins from cell metabolism based on tunable aptamer and microchip electrophoresis. Biosens. Bioelectron. 63, 105-111.

Lin, X., Chen, Q., Liu, W., Zhang, J., Wang, S., Lin, Z., Lin, J.M., 2015b. Oxygen-induced cell migration and on-line monitoring biomarkers modulation of cervical cancers on a microfluidic system. Sci. Rep. 5, 9643-9649.

Malhotra, R., Patel, V., Chikkaveeraiah, B.V., Munge, B.S., Cheong, S.C., Zain, R.B., Abraham, M.T., Dey, D.K., Gutkind, J.S., Rusling, J.F., 2012. Ultrasensitive detection of cancer biomarkers in the clinic by use of a nanostructured microfluidic array. Anal. Chem. 84(14), 6249-6255.

Maxwell, P.J., Gallagher, R., Seaton, A., Wilson, C., Scullin, P., Pettigrew, J., Stratford, I.J., Williams, K.J., Johnston, P.G., Waugh, D.J., 2007. HIF-1 and NF-kappaB-mediated upregulation of CXCR1 and CXCR2 expression promotes cell survival in hypoxic prostate cancer cells. Oncogene 26(52), 7333-7345.

Munge, B.S., Coffey, A.L., Doucette, J.M., Somba, B.K., Malhotra, R., Patel, V., Gutkind, J.S., Rusling, J.F., 2011. Nanostructured immunosensor for attomolar detection of cancer biomarker interleukin-8 using massively labeled superparamagnetic particles. Angew. Chem. Int. Ed. Engl. 50(34), 7915-7918.

Nassar, A.F., Williams, B.J., Yaworksy, D.C., Patel, V., Rusling, J.F., 2016. Rapid label-free profiling of oral

cancer biomarker proteins using nano-UPLC-Q-TOF ion mobility mass spectrometry. Proteomics Clin. Appl. 10(3), 280-289.

Ouchi, R., Okabe, S., Migita, T., Nakano, I., Seimiya, H., 2016. Senescence from glioma stem cell differentiation promotes tumor growth. Biochem. Biophys. Res. Commun. 470(2), 275-281.

Ricci-Vitiani, L., Pallini, R., Biffoni, M., Todaro, M., Invernici, G., Cenci, T., Maira, G., Parati, E.A., Stassi, G., Larocca, L.M., De Maria, R., 2010. Tumour vascularization via endothelial differentiation of glioblastoma stem-like cells. Nature 468(7325), 824-828.

Rusling, J.F., Kumar, C.V., Gutkind, J.S., Patel, V., 2010. Measurement of biomarker proteins for point-of-care early detection and monitoring of cancer. Analyst 135(10), 2496-2511.

Sarkar, S., Sabhachandani, P., Konry, T., 2016. Isothermal Amplification Strategies for Detection in Microfluidic Devices. Trends Biotechnol. 35(3), 186-189.

Shi, J., Wei, P.K., 2016. Interleukin-8: A potent promoter of angiogenesis in gastric cancer. Oncol. Lett. 11(2), 1043-1050.

Soda, Y., Hanahan, D., 2011. Transdifferentiation of glioblastoma cells into vascular endothelial cells. Proc. Natl. Acad. Sci. U. S. A. 108(11), 4274-4280.

Stobiecka, M., Chalupa, A., Dworakowska, B., 2016. Piezometric biosensors for anti-apoptotic protein survivin based on buried positive-potential barrier and immobilized monoclonal antibodies. Biosens Bioelectron 84, 37-43.

Stobiecka, M., Hepel, M., 2011. Effect of buried potential barrier in label-less electrochemical immunodetection of glutathione and glutathione-capped gold nanoparticles. Biosens Bioelectron 26(8), 3524-3530.

Sung, H.J., Choi, S., Lee, J.W., Ok, C.Y., Bae, Y.S., Kim, Y.H., Lee, W., Heo, K., Kim, I.H., 2014. Inhibition of human neutrophil activity by an RNA aptamer bound to interleukin-8. Biomaterials 35(1), 578-589.

Toh, S.Y., Citartan, M., Gopinath, S.C., Tang, T.H., 2015. Aptamers as a replacement for antibodies in enzyme-linked immunosorbent assay. Biosens. Bioelectron. 64, 392-403.

Torrente-Rodriguez, R.M., Campuzano, S., Ruiz-Valdepenas Montiel, V., Gamella, M., Pingarron, J.M., 2016. Electrochemical bioplatforms for the simultaneous determination of interleukin (IL)-8 mRNA and IL-8 protein oral cancer biomarkers in raw saliva. Biosens. Bioelectron. 77, 543-548.

Wan, Y., Deng, W., Su, Y., Zhu, X., Peng, C., Hu, H., Peng, H., Song, S., Fan, C., 2011. Carbon nanotube-based ultrasensitive multiplexing electrochemical immunosensor for cancer biomarkers. Biosens. Bioelectron. 30(1), 93-99.

Waugh, D.J., Wilson, C., 2008. The interleukin-8 pathway in cancer. Clin. Cancer Res. 14(21), 6735-6741.

Wei, F., Patel, P., Liao, W., Chaudhry, K., Zhang, L., Arellano-Garcia, M., Hu, S., Elashoff, D., Zhou, H., Shukla, S., Shah, F., Ho, C.M., Wong, D.T., 2009. Electrochemical sensor for multiplex biomarkers detection. Clin. Cancer Res. 15(13), 4446-4452.

Yang, C.Y., Brooks, E., Li, Y., Denny, P., Ho, C.M., Qi, F., Shi, W., Wolinsky, L., Wu, B., Wong, D.T., Montemagno, C.D., 2005. Detection of picomolar levels of interleukin-8 in human saliva by SPR. Lab Chip 5(10), 1017-1023.

Zhao, Y., Dong, J., Huang, Q., Lou, M., Wang, A., Lan, Q., 2010. Endothelial cell transdifferentiation of human glioma stem progenitor cells in vitro. Brain Res. Bull. 82(5-6), 308-312.

## Figure captions

**Fig. 1.** Principle of cell observation and detection of IL-8 by RCA and fluorescence probe under hypoxia condition on the microchip. (A) Schematic diagram of the proposed fluorescence detection method of IL-8. (B) The design of dual function microfluidic chip. (C) Hypoxia signal pathway in TDECs and HUVECs.

**Fig. 2.** Identification of GSCs and TDECs. (A) merged fluorescence image of glioma stem-like cells, stained for CD133 (in red), nestin (in green), DAPI (in blue). (B) Fluorescence image of U87MG, stained for CD31 (in red), DAPI (in blue), 10× objective lens. (C) Fluorescence image of TDECs, stained for CD31 (in red), DAPI (in blue), 20× objective lens. (D) Fluorescence image of TDECs, stained for CD31 (in red), DAPI (in blue), 10× objective lens.

**Fig. 3.** AFM image of modified glass surface. (A) The process of chip modification. (B) AFM image of the blank glass surface. (C) AFM image of glass surface modified by APTES. (D) AFM image of glass surface modified by glutaraldehyde. (E) Glass surface modified by APTES, glutaraldehyde and IL-8 antibody.

**Fig. 4.** Analysis of the amplification effect of RCA. (A) Chip electrophoresis results of RCA reactant. (B) Chip electrophoresis results of RCA reactant and exonuclease I. (C) Chip electrophoresis results of RCA product. (D) Chip electrophoresis results of RCA product and exonuclease I. (E) The fluorescence image of IL-8 detection channel without RCA. (F) The fluorescence image of IL-8 detection channel with RCA.The concentration of IL-8 is 60 pg $mL^{-1}$.

**Fig. 5.** Optimization of antibody, IL-8, aptamer sequence by BLI. (A) BLI result of aptamer-IL-8-antibody sequence. The short horizontal line indicates the binding buffer washing and balancing time. (B) BLI result of antibody -IL-8-aptamer sequence. The short horizontal line indicates the binding buffer washing and balancing time.

**Fig. 6.** Detection of the standard sample of IL-8. (A) Fluorescence image of microchip channel and fluorescence intensity statistics obtained by ImageJ software for different IL-8 concentration. (B) The standard curve of lower concentration of IL-8. (C) Specific validation of the method achieved by the detection of IL-8 (0.1 nM) and other proteins(1nM) except for ATP(20 nM) and EGF(3 nM),

**Fig. 7.** Analysis of IL-8 in cell culture medium. (A) Fluorescence image of detection channel and cell culture channel in the microchip. (B) IL-8 concentration in HUVEC and TDEC culture medium with and without DFO treating by proposed method and ELISA. (C) Semi-quantitative analysis of the IL-8 concentration of HUVEC in 10% FBS containing culture medium by proposed method and ELISA.

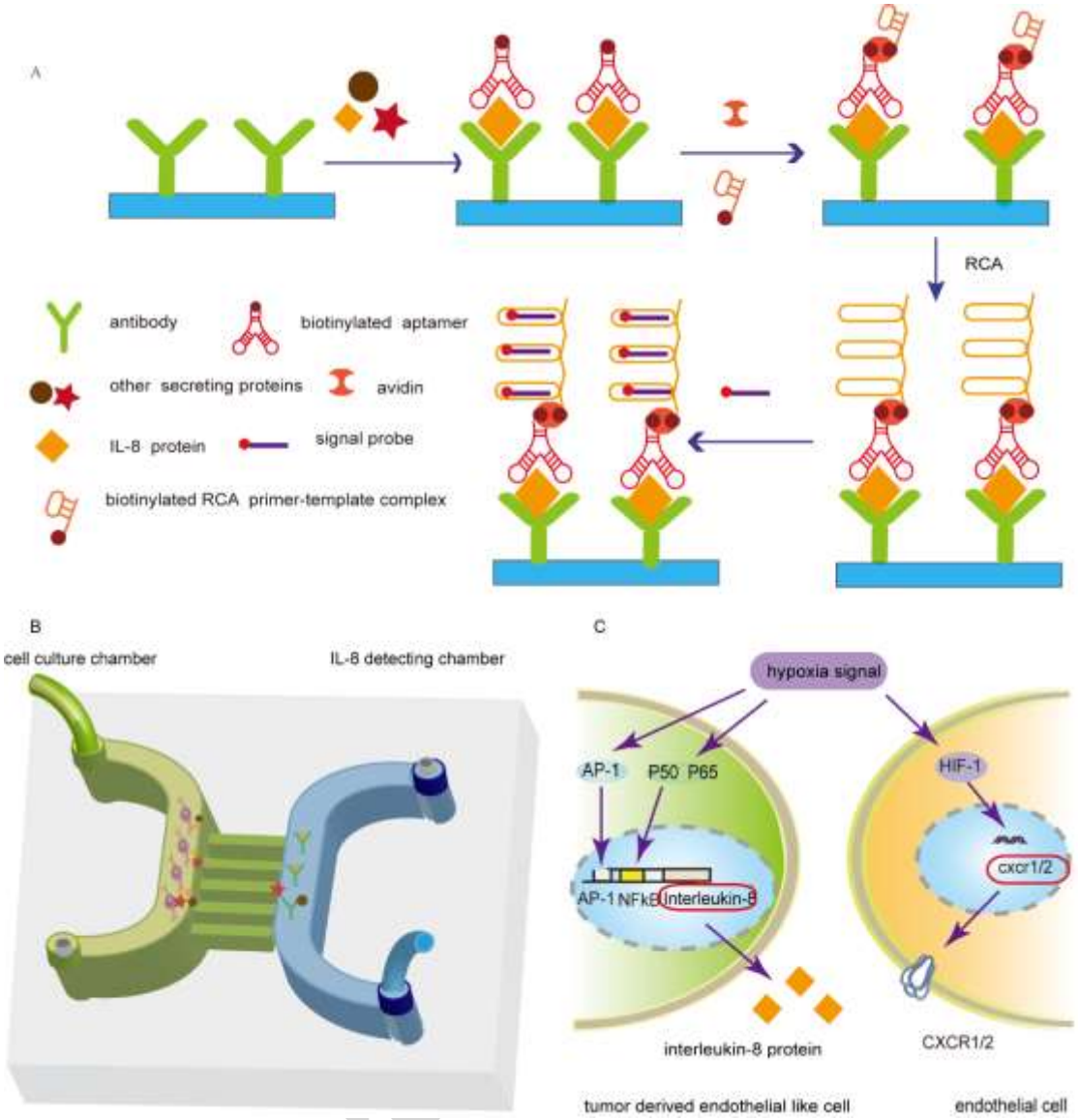


**Figure 1**

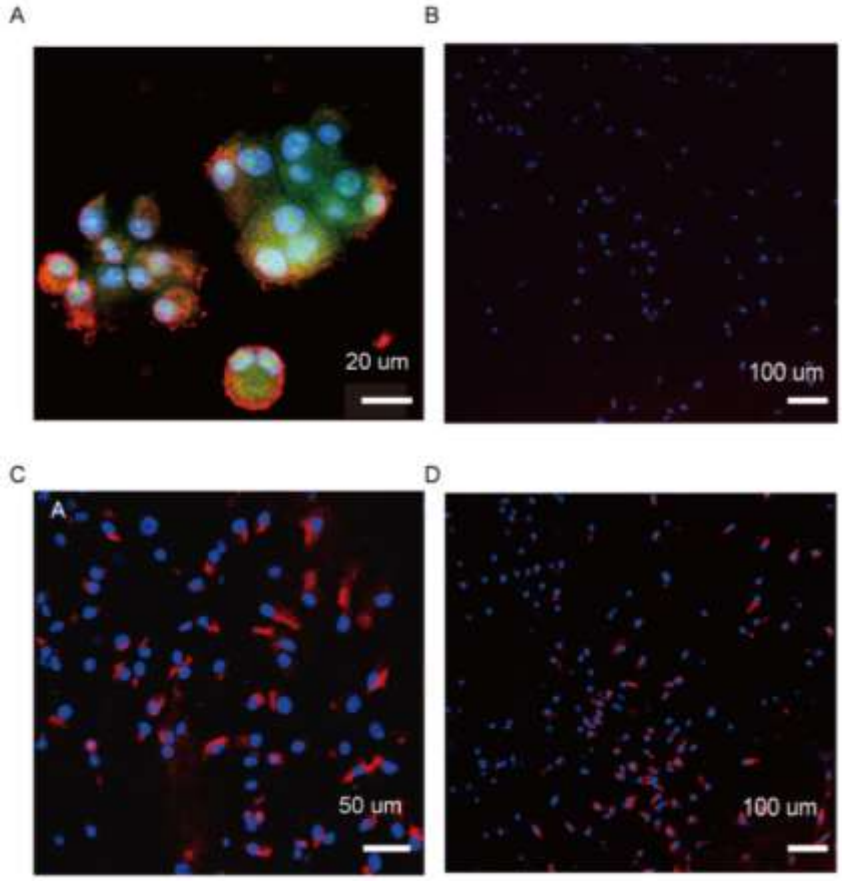


**Figure 2**

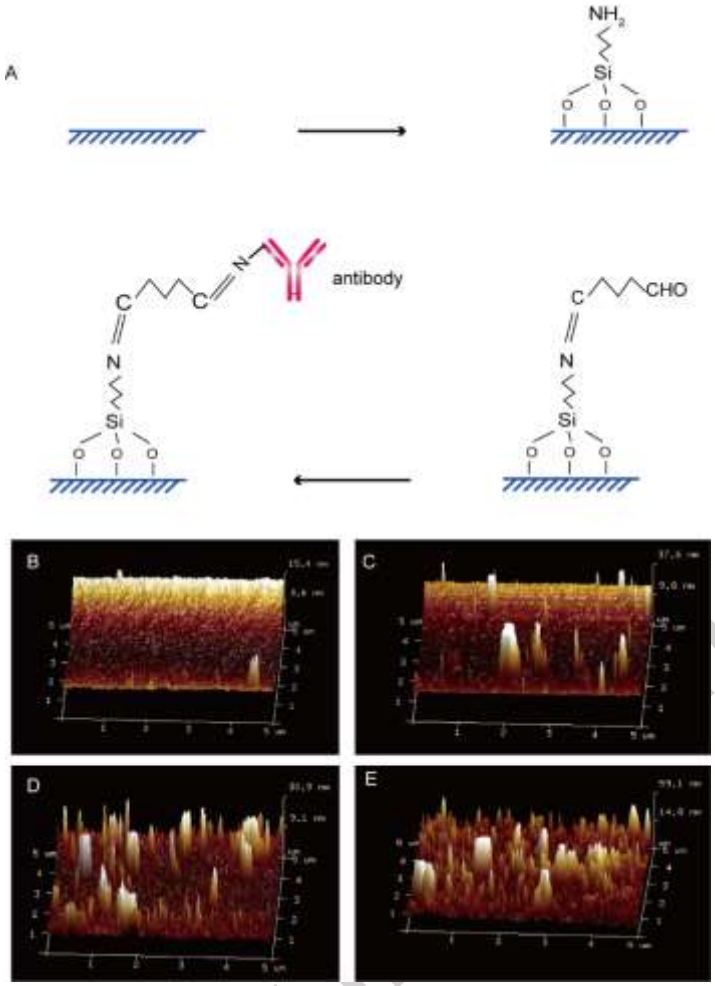


**Figure 3**

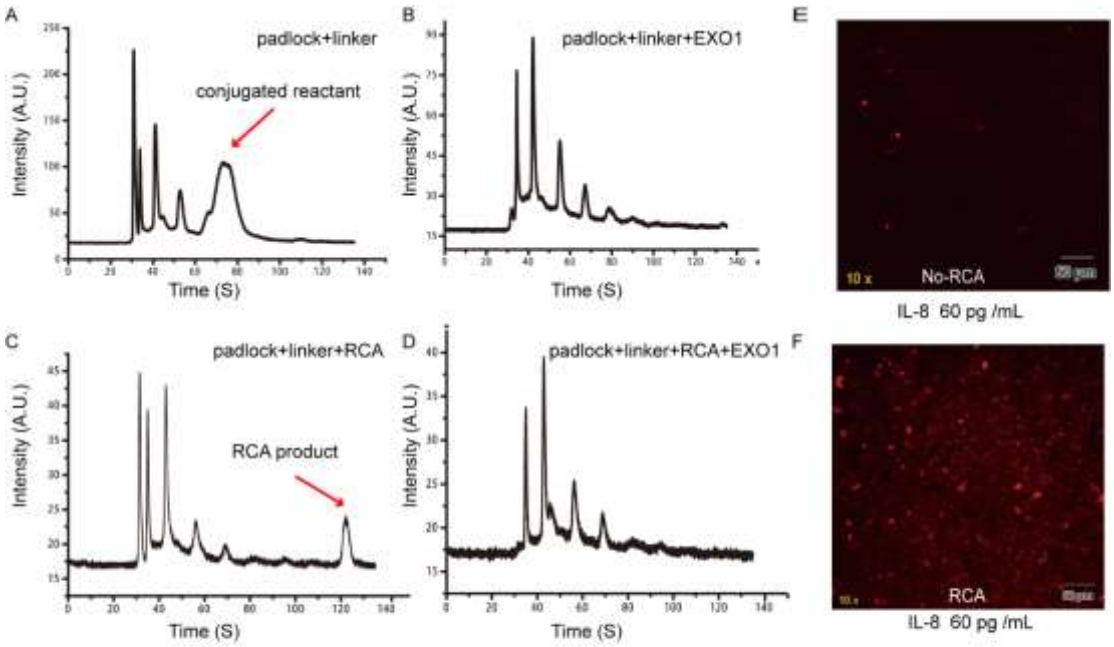


**Figure 4**

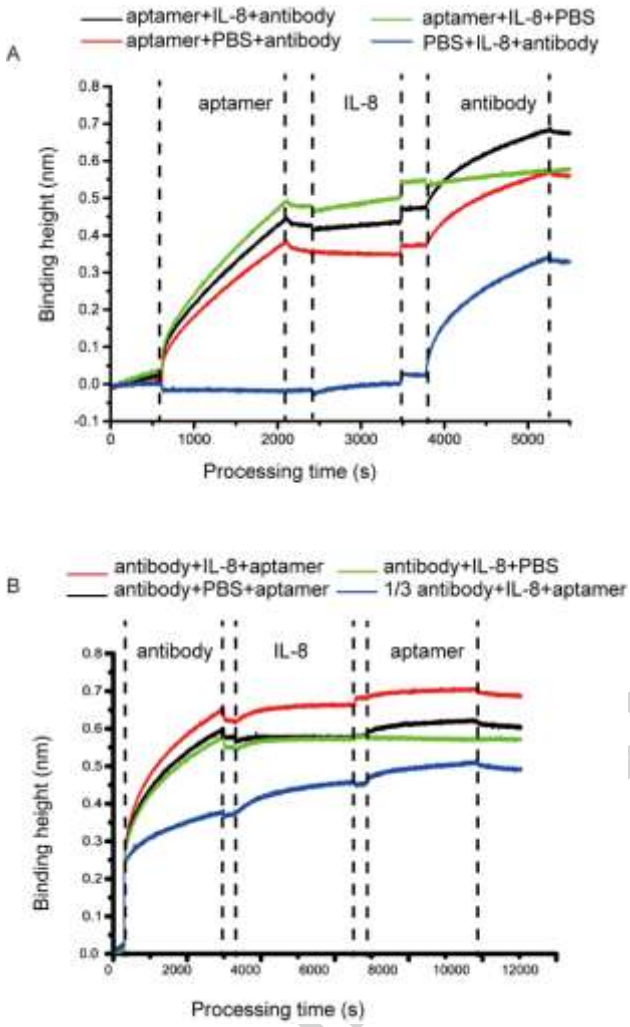


**Figure 5**

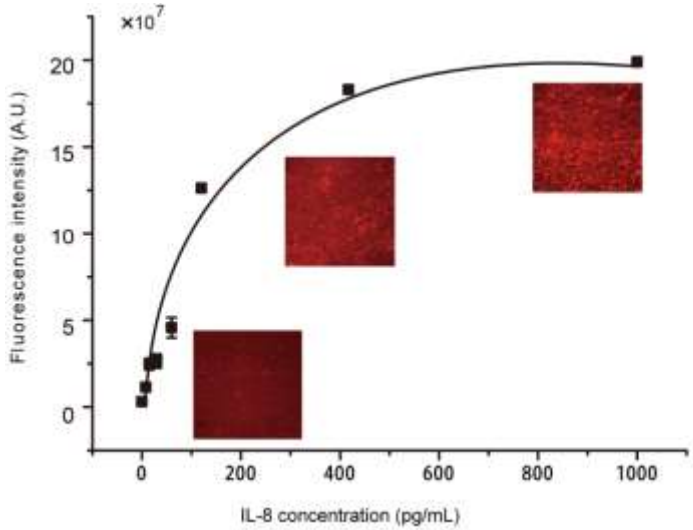
×10^7
Fluorescence intensity (A.U.)
IL-8 concentration (pg/mL)

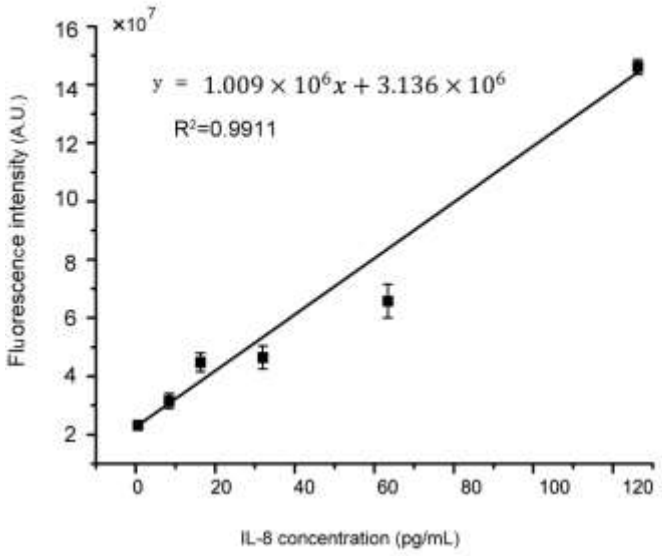
×10^7
y = 1.009 × 10^6 x + 3.136 × 10^6
R²=0.9911
Fluorescence intensity (A.U.)
IL-8 concentration (pg/mL)

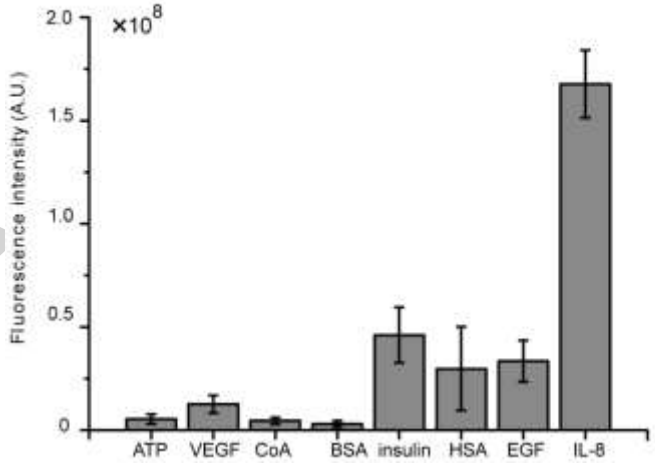
×10^8
Fluorescence intensity (A.U.)
ATP
VEGF
CoA
BSA
insulin
HSA
EGF
IL-8

**Figure 6**

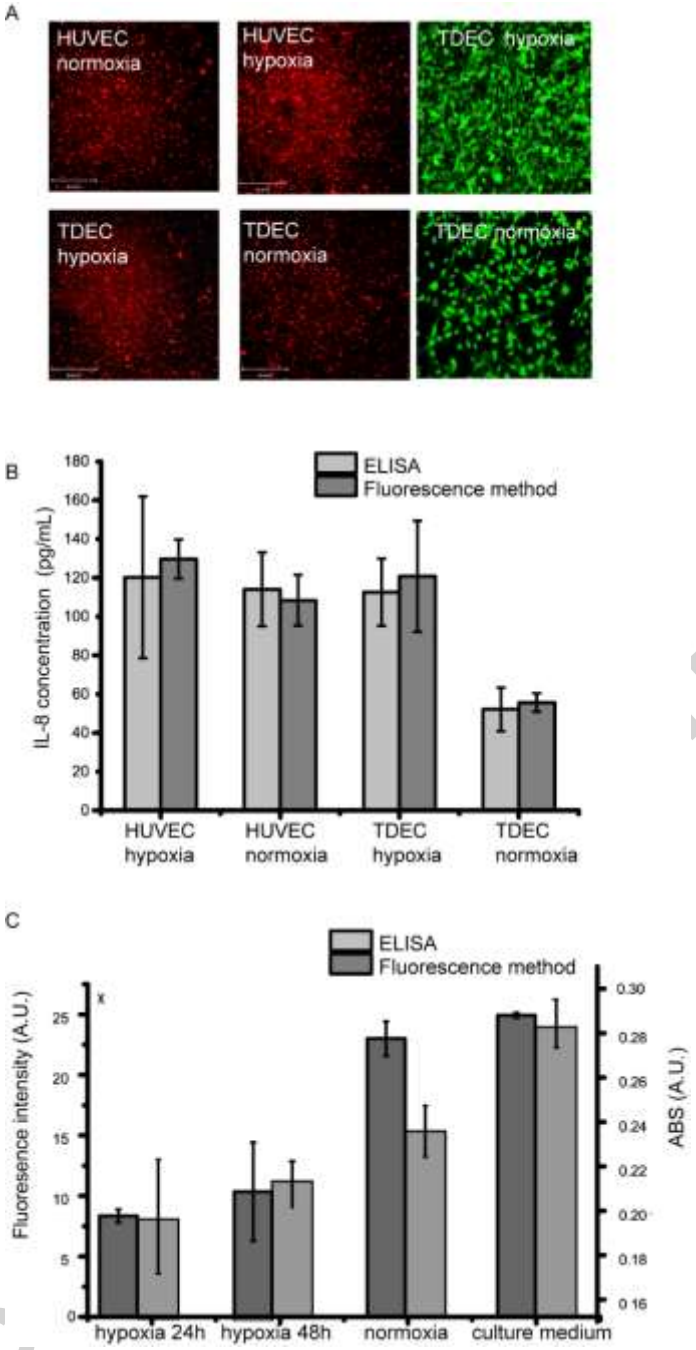
A
HUVEC normoxia
HUVEC hypoxia
TDEC hypoxia
TDEC hypoxia
TDEC normoxia
TDEC normoxia
B
ELISA
Fluorescence method
IL-8 concentration (pg/mL)
HUVEC hypoxia
HUVEC normoxia
TDEC hypoxia
TDEC normoxia
C
ELISA
Fluorescence method
Fluoresence intensity (A.U.)
ABS (A.U.)
hypoxia 24h
hypoxia 48h
normoxia
culture medium

**Figure 7**

# Highlights

1) LOD readout of interleukin-8 is 7.5 pg $mL^{-1}$.

2) Cell morphology and online protein detection is monitored at the same time.

3) Aptamer, interleukin-8 and antibody system is established and optimized.

4) The signal amplification is achieved by the rolling circle amplification.